



HAL
open science

Study on friction and wear behavior of polyphenylene sulfide composites reinforced by short carbon fibers and sub-micro TiO particles

Zhenyu Jiang, Lada Antonova Gyurova, Alois K. Schlarb, Klaus Friedrich,
Zhong Zhang

► To cite this version:

Zhenyu Jiang, Lada Antonova Gyurova, Alois K. Schlarb, Klaus Friedrich, Zhong Zhang. Study on friction and wear behavior of polyphenylene sulfide composites reinforced by short carbon fibers and sub-micro TiO particles. *Composites Science and Technology*, 2009, 68 (3-4), pp.734. 10.1016/j.compscitech.2007.09.022 . hal-00563489

HAL Id: hal-00563489

<https://hal.science/hal-00563489>

Submitted on 6 Feb 2011

HAL is a multi-disciplinary open access archive for the deposit and dissemination of scientific research documents, whether they are published or not. The documents may come from teaching and research institutions in France or abroad, or from public or private research centers.

L'archive ouverte pluridisciplinaire **HAL**, est destinée au dépôt et à la diffusion de documents scientifiques de niveau recherche, publiés ou non, émanant des établissements d'enseignement et de recherche français ou étrangers, des laboratoires publics ou privés.

Accepted Manuscript

Study on friction and wear behavior of polyphenylene sulfide composites reinforced by short carbon fibers and sub-micro TiO₂ particles

Zhenyu Jiang, Lada Antonova Gyurova, Alois K. Schlarb, Klaus Friedrich, Zhong Zhang

PII: S0266-3538(07)00419-8
DOI: [10.1016/j.compscitech.2007.09.022](https://doi.org/10.1016/j.compscitech.2007.09.022)
Reference: CSTE 3870

To appear in: *Composites Science and Technology*

Received Date: 17 April 2007
Revised Date: 6 September 2007
Accepted Date: 6 September 2007

Please cite this article as: Jiang, Z., Gyurova, L.A., Schlarb, A.K., Friedrich, K., Zhang, Z., Study on friction and wear behavior of polyphenylene sulfide composites reinforced by short carbon fibers and sub-micro TiO₂ particles, *Composites Science and Technology* (2007), doi: [10.1016/j.compscitech.2007.09.022](https://doi.org/10.1016/j.compscitech.2007.09.022)

This is a PDF file of an unedited manuscript that has been accepted for publication. As a service to our customers we are providing this early version of the manuscript. The manuscript will undergo copyediting, typesetting, and review of the resulting proof before it is published in its final form. Please note that during the production process errors may be discovered which could affect the content, and all legal disclaimers that apply to the journal pertain.



Study on friction and wear behavior of polyphenylene sulfide composites reinforced by short carbon fibers and sub-micro TiO₂ particles

Zhenyu Jiang^{1,*}, Lada Antonova Gyurova¹, Alois K. Schlarb¹, Klaus Friedrich^{1,2},
Zhong Zhang³

¹Institute for Composite Materials (Institut für Verbundwerkstoffe GmbH), University of Kaiserslautern, 67663 Kaiserslautern, Germany

²School of Aerospace, Mechanical and Mechatronic Engineering, The University of Sydney, Sydney, NSW 2006, Australia

³National Center for Nanoscience and Technology, China, 100080 Beijing, China

Abstract

Polyphenylene sulfide (PPS) composites filled with short carbon fibers (SCFs) (up to 15 vol.%) and sub-micro-scale TiO₂ particles (up to 7 vol.%) were prepared by extrusion and subsequently injection-molding. Based on the results of sliding wear tests, the tribological behavior of these materials was investigated using an artificial neural network (ANN) approach. A synergistic effect of the incorporated short carbon fibers and sub-micro TiO₂ particles is reported. The lowest specific wear rate was obtained for the composition of PPS with 15 vol.% SCF and 5 vol.% TiO₂. A more optimal composition of PPS with 15 vol.% SCF and 6 vol.% TiO₂ was estimated according to ANN prediction. The scanning electron microscopy (SEM) observation revealed that this hybrid reinforcement could be interpreted in terms of a positive rolling effect of the particles between the two sliding surfaces, which protected the short carbon fibers from being pulled out of the PPS matrix.

Keywords: A. Short-fiber composites; A. Particle-reinforced composites; B. Friction/wear; D. Scanning electron microscopy; Artificial neural network

1 Introduction

Polymer composites occupy a considerable market share nowadays as one of the most common engineering materials. They provide a combination of various advantages, such as ease in manufacturing, cost effectiveness and excellent performance, which

* Corresponding author. Tel.: +49 631 2017289; fax: +49 631 2017196.
E-mail address: zhenyu.jiang@ivw.uni-kl.de (Z. Jiang).

cannot be attained by metals, ceramics, or polymers alone [1]. In recent years a tremendous interest was raised in scientific and industrial communities to apply polymer composites in sliding components, where their self lubricating properties can be exploited to avoid the need for oil or grease lubrication accompanied with the problems of contamination [2].

The choice of an appropriate matrix is of great importance in the design of wear resistant polymer composites. The required properties of such a tribo-matrix includes high service temperature, good chemical resistance and outstanding cohesive strength [3]. Within this frame, PPS is regarded as a proper tribo-matrix material [4]. Neat PPS, however, is a brittle material with relatively low impact strength [5]. Therefore, various fillers have been incorporated in order to enhance the property profile of PPS. Short carbon fibers (SCFs), which are widely advocated as a decisive reinforcement component, show a remarkable capability to increase the wear resistance of PPS [6]. As for the incorporation of particulate fillers, the problem becomes more sophisticated. Some micro-particles such as Ag_2S , CuS , NiS , SiC and Cr_3C_2 have been reported to improve the wear resistance of PPS, but others like PbTe , PbSe , ZnF_2 , SnS and Al_2O_3 have been found to exercise an adverse influence [7-12]. The concept of adding particles of sub-micro- or nano-scale into polymers is one of the most intriguing subjects in the recent decades. On the one hand, the action of the particle angularity, which is detrimental to the wear resistance, is greatly diminished on those scales. On the other hand, proper particulate nano-fillers contribute positively towards the development of a thin and uniform transfer film and the better adhesion of transfer film to the counterpart during sliding [13, 14], which play a crucial role in the enhancement of wear resistance [15]. However, there are few papers that investigated the influence of the hybrid reinforcement of sub-micro/nano-particles and short carbon fibers on the tribological behavior of polymer composites [16-18]. Very recently, Cho and Bahadur [19] reported that a lower wear rate was attained in the case that nano CuO particles and short carbon/aramid fibers were added into PPS, as compared to that including one of the two fillers alone.

The objective of the present study is to investigate on the tribological behavior of PPS composites filled with short carbon fibers and sub-micro TiO_2 particles. An artificial neural network (ANN) approach, a powerful analytical tool, is introduced to

model the functional relationship between the wear properties of PPS composites and the chosen parameters, including material compositions and testing conditions. According to the visualized profiles of the wear properties predicted by the ANNs, an optimal combination of short carbon fibers and sub-micro TiO₂ particles could be obtained to fulfill the hybrid reinforcement, which significantly improves the wear resistance of PPS composites. Moreover, the wear mechanism for the synergistic effect of the two kinds of fillers was also studied based on the SEM analysis of the surfaces of sliding bodies.

2 Experimental

Polyphenylene-sulfide (Fortron 214 C, Ticona GmbH) was used as a matrix material. Pitch-based short carbon fibers (Kureha M-2007S, Kureha Chemicals GmbH) and TiO₂ (Kronos 2310, Kronos Titan GmbH) were selected as fillers. The total content of the fillers in the matrix was up to 22 vol.%. The average diameter and length of the short carbon fiber were approximately 14.5 μm and 90 μm, respectively. The average size of TiO₂ sub-micro-particle is about 300 nm.

The compounding of the fillers with the matrix was achieved via twin screw extruder (ZE25Ax44D, Berstorff). The compounds were further molded into plates (80×80×4 mm³) using an injection molding machine (Allrounder, Arburg GmbH). For the purpose of testing, samples were cut into pins with a contact surface of 4×4 mm². In order to ensure identical flow conditions, only the middle section of the plates were chosen for machining the samples.

Sliding wear tests were completed on a pin-on-disc set-up under different *pν*-conditions at room temperature. The counterpart (steel disc 100Cr6, LS 2542, INA Scheffler KG) was cleaned with acetone prior to test. The surface roughness of the counterpart was measured as average roughness $R_a = 0.19$ μm and peak-to-valley roughness $R_t = 2.20$ μm respectively using a Mahr Perthometer (Perthen, Mahr-Perthen). The applied pressure was varied between 1 and 3 MPa, the sliding speed was set as 1 or 3 m/s, and the testing time was fixed at 20 hours. For some of the materials, e.g. neat PPS, the test was stopped after 1 hour due to the severe wear. In the course of the experiments both the normal and frictional forces were recorded to determine the friction coefficient. The specific wear rate, w_s , was calculated by the following equation:

$$w_s = \frac{\Delta m}{\rho \cdot v \cdot t \cdot F_N} \quad [mm^3 / Nm] \quad (1)$$

where Δm is the mass loss, ρ is the density of the material, v is the sliding speed, and t is the duration of test. F_N represents the normal force imposed on the specimen during sliding.

Since the two testing parameters, i.e. the sliding speed v and the applied pressure p ($p = \frac{F_N}{\text{Contact area}}$), are changed independently, a time related depth wear rate, w_t , is

introduced to evaluate the wear behavior under various pv -conditions.

$$w_t = w_s \cdot p \cdot v = \frac{\Delta h}{t} \quad [mm / s] \quad (2)$$

where Δh represents the height reduction of the specimen after the test.

Finally the morphologies of selected worn pins and wear tracks were examined by scanning electron microscopy (SEM) (Jeol 6300, Jeol).

3 Artificial neural network analysis

3.1 Principle

The ANN technology is inspired by the biological neural system, and has been used to solve a wide variety of problems in diverse fields (see Reference [20-22] for the reviews about its application in material science). ANN is ideally suitable for some complex, non-linear and multi-dimensional problems because it is able to imitate the learning capability of human. This means the network can learn directly from the examples without any prior formulae about the nature of the problem, and generalize by itself some knowledge, which could be applied for new cases. A neural network is a system composed of many cross linked simple processing units, also called neurons. As illustrated in Fig. 1, a neural network is generally defined as three parts connected in series: input layer, hidden layer and output layer [23]. The coarse information is accepted by the input layer, and processed in the hidden layer. Finally the results are exported via the output layer. For convenience, the structure of the neural network is described as the following notation:

$$N_{in} - [N_1 - N_2 - \dots - N_h]_h - N_{out} \quad (3)$$

where N_{in} and N_{out} represent the number of neurons in the input and output layer, respectively. N_h is the number of neurons in each hidden layer, and h denotes the

amount of hidden layers. The neurons in the contiguous layers are cross-linked by the weighted inter-connections, which resemble the bioelectricity passing through the real axons. Besides the weight, the neurons also have a bias value, which refers to their initial states. During the training process, the generalized knowledge is memorized in terms of the combination of weights and biases. In the hidden layers and the output layer, the individual neuron gets the information from the neurons in the previous layer, and modulates the information with a transfer function, weight as well as bias, and then outputs the result.

The neural network in this study is operated by a backpropagation algorithm, which is one of the most widely used algorithms for multi-layer perceptron. The weights and biases are initialized as small random values. Then the network is fed with a series of training data. During an iterative training process, the weights and biases are adjusted by the network itself to optimize its performance, namely to minimize the difference between output values and real values. A quadratic form is used as the performance function:

$$E = \frac{1}{2L} \sum_{t=1}^L [d(t) - p(t)]^2 \quad (4)$$

where L refers to the number of training patterns, $d(t)$ is the desired output value, and $p(t)$ is the target output value predicted by the ANN for the t th pattern. During the training process, the network is presented with the data for hundreds of cycles, the weights and biases are adjusted until the expected error level is achieved or the maximum iteration is reached. This iterative adjustment of the weights and biases follows the equations

$$\begin{aligned} W_{ji}^{(n)}(k) &= W_{ji}^{(n)}(k-1) - \alpha \frac{\partial E}{\partial W_{ji}^{(n)}} \\ b_j^{(n)}(k) &= b_j^{(n)}(k-1) - \alpha \frac{\partial E}{\partial b_j^{(n)}} \end{aligned} \quad (5)$$

where α represents the learning rate, and k refers to the iteration.

3.2 Procedure

Table 1 lists the chosen input variables (material compositions and testing conditions) and the output variables (specific wear rate and friction coefficient), as well as the range of the experimental values. The prediction quality of ANN has been proved to be sensitive to the size of the database for network-training. Thus a larger experimental

database including 66 groups of independent tests, in which the compositions contain lubricant fillers (graphite and PTFE) in addition to short carbon fibers and TiO_2 , were used in the present study to train the network. Based on our previous methodology research [24, 25], two networks with the structures of 7-[9-3]₂-1 and 7-[3-1]₂-1 were selected by training and testing process in this study. The former is employed to model the relation between the specific wear rate and the chosen input variables. The latter is used for the friction coefficient. A Powell-Beale conjugate gradient algorithm [26] was chosen as the learning algorithm.

4 Results

4.1 Effect of short carbon fibers and TiO_2 particles on wear and friction

Fig. 2a shows both the measured and the predicted results of the specific wear rate versus the volume content of short carbon fibers and TiO_2 particles. It can be seen that the sole incorporation of TiO_2 particles leads to an increase in specific wear rate w_s . The significant reductions (by a factor of 10^2) in w_s show that short carbon fibers plays a key role in improving the wear resistance of PPS, both as a single or a second reinforcement phase. This improvement, however, tends to a saturation state when the content of short carbon fiber exceeds 10 vol.%. When both of short carbon fibers and TiO_2 particles are incorporated to PPS matrix, a hybrid reinforcement effect can be found. For both 10 vol.% and 15 vol.% short carbon fibers, the specific wear rate exhibited a drop-off tendency with the increase of TiO_2 content in the range 3-7 vol.%. According to the experimental results the composition of PPS with 15 vol.% SCF and 5 vol.% TiO_2 gives the highest wear resistance. Furthermore, it is estimated from the predicted trends that the lowest specific wear rate can be obtained for PPS with 15 vol.% SCF and 6 vol.% TiO_2 . Fig. 2b shows the trend of measured and predicted friction coefficient. In comparison to the specific wear rate, both two fillers result in a monotonic decrease in friction coefficient. Although the mechanisms of the reduction in friction coefficient contributed by each of the two fillers are different, which will be discussed in section 5, it is clear that they can work simultaneously and make the respective effects superposed.

4.2 Influence of testing conditions on tribological behavior

Fig. 3 displays the ANN predicted 3D profiles of the specific wear rate and the friction coefficient as function of the sliding speed and the applied pressure for PPS with 15 vol.% SCF and 5 vol.% TiO_2 . The measured data are plotted as the black points

with error bars. In Fig. 3a, the specific wear rate increases obviously with the increase in applied pressure at low sliding speed (1 m/s), whereas it becomes less sensitive to the applied pressure at high sliding speed (3 m/s). Fig. 3b shows the variation of friction coefficient versus the testing conditions. The friction coefficient exhibits a monotonic decrease trend when either sliding speed or applied pressure was increased. It can be estimated that a relatively lower value will be achieved under the pv -conditions of 3×3 MPa·m/s ($3 \text{ MPa} \times 3 \text{ m/s}$). However, the stick-slip phenomenon occurred during the experiments under this condition and resulted in that the friction coefficient can not be accurately determined.

When plotting the results in terms of the depth wear rate w_t (Fig. 4), one can see according to the fitting curve that w_t increases with the product of applied pressure and sliding speed in a quasi-linear fashion, at a slope which corresponds to an average specific wear rate of $0.7 \times 10^{-6} \text{ mm}^3/\text{Nm}$ over a pv -product of 9 MPa·m/s. Only under the pv -conditions of 3×1 MPa·m/s, there is a remarkable deviation from the fitting curve.

5 Discussions

5.1 Hybrid reinforcement: short carbon fibers and sub-micro TiO_2 particles

The mechanical properties of multi-phase materials can be generally considered as a function of the respective contribution of each phase [27]. The situation is more complicated with regard to the wear behavior, since some chemical reactions and physical interactions among these phases may occur during the wear process and dominate the wear performance of polymer composites. It is well known that short carbon fibers serve as a fundamental load bearing element in the wear process of polymer composites [6, 28]. Moreover, they have a lubricating function and enhance the thermal conductivity of matrix [29]. Generally, the wear process of short carbon fiber reinforced composites can be summarized in the following stages: (i) after wear of the matrix material on and around the fibers, (ii) the fibers get exposed to the counterpart asperities, and are thinned down. (iii) Subsequently they get cracked, eventually pulverized and removed, or pulled-out from matrix [30]. These mechanisms can be recognized in the SEM microphotograph of the worn surfaces, as displayed in Fig. 5a. In Fig. 5b, the wear grooves and the material fragments indicate that the solely incorporated sub-micro TiO_2 particles, in particular at high content, result in a severer wear, though the hard particles also help to develop the toughness and stiffness of the

matrix to some extent. This effect is ascribed to that the particles act as an abrasive third body and meanwhile increase the discontinuities in matrix. The combination of the two kinds of fillers, however, promotes a pronounced change in wear process. It can be seen in Fig. 5c that a considerable amount of compacted wear debris are collected around the fibers, acting temporarily as a distance holder between the composite pin and the steel counterpart, and thus protect the fibers. Furthermore, the matrix is much smoother with fewer small scratches in comparison to the PPS filled with short carbon fibers alone. An additional positive effect of the sub-micro-particles is considered to be occurring. The sub-micro TiO_2 particles, when being used in combination with the much larger short carbon fibers, are not easily ploughed out of the matrix by counterpart asperities. Instead, they are gradually released and likely start to act as a rolling body between the two mating surfaces. As illustrated in Fig. 6a, the effect of sub-micro-particles may involve two aspects:

1. The rolling action of sub-micro-particles protects the short carbon fibers, especially at their edges, from being easily pulled out of the matrix [18]. Moreover, the particles can polish the exposed fiber surfaces during the sliding, since they are slightly harder than short carbon fibers. In this way, they reduce the hard abrasion between the two contact surfaces to mild one.
2. The sub-micro-particles, either operating alone or being wrapped by the matrix material, act as a ball-bearing component, which means that the particles roll rather than slide between the two mating surfaces, and reduce the shear stress, the friction coefficient and the contact temperature. This concept was also reported with the fullerene-like WS_2 nano-particles as additives for lubrication fluids [31].

Fig. 6(b-e) elucidate the positive rolling effect of sub-micro-particles in detail, which can be divided into four stages. (i) During the wear the particles are ploughed out by the counterpart tip together with matrix material. These complexes play a role as a rolling third body between the hard metal disk and the soft polymer composite pin (Fig. 6b). (ii) When counterpart tip comes to the front edge of fiber, the complexes prevent the tip from directly scraping the fiber (Fig. 6c). Meanwhile, they are hindered by the exposed fiber and accumulate there. (iii) The particles become an abrasive component and polish the fiber surface (Fig. 6d). (iv) Finally, the counterpart tip moves through the whole surface of fiber, sometimes damaging the back edge of the fiber (Fig. 5c.), and then

starts to plough the soft matrix again (Fig. 6e).

5.2 Wear under high $p\nu$ -conditions

The wear of materials usually becomes severer under high $p\nu$ -conditions. However, sliding speed and applied pressure has different influence on the wear behavior. In the present work, the rise in sliding speed leads to a relatively gentler increase of wear in comparison with that in applied pressure. As already shown in Fig. 4, $p\nu$ -condition of 3×1 MPa·m/s leads to a higher depth wear rate than that at 1×3 MPa·m/s or even 2×3 MPa·m/s. It is believed that this phenomenon is related to the contact temperature in the process of wear, which is mainly controlled by the sliding speed. Table 2 lists the maximum value of contact temperature under different $p\nu$ -conditions for PPS with 15 vol.% SCF and 5 vol.% TiO₂. This peak temperature generally occurs at the early stage of wear, accompanied with the peak of friction coefficient. It is found that the maximum contact temperatures at $p\nu$ -product of 2×3 MPa·m/s and 3×3 MPa·m/s reach 113.9 °C and 120.1 °C respectively, which are higher than the glass transition temperature of the PPS composite (110.3 °C, measured by dynamic mechanical thermal analysis (DMTA)). This indicates that under these $p\nu$ -conditions the PPS matrix on the surface of the composite pin can easily deform plastically when transfer film is initialized on the counterpart surface, and contribute to develop a compact and smooth transfer film with better adhesion to the disk. In consequence, the wear was reduced from hard abrasion to milder one.

Fig. 7 gives the SEM micrographs of the worn surface of PPS with 15 vol.% SCF and 5 vol.% TiO₂ and the corresponding wear track on the steel counterpart at different $p\nu$ -products ((a-b) 3×1 MPa·m/s; (c-d) 2×3 MPa·m/s). It can be seen that the worn surface of the sample at $p\nu$ -product of 2×3 MPa·m/s (Fig. 7c) is much smoother than that at $p\nu$ -product of 3×1 MPa·m/s (Fig. 7a). Despite much higher sliding speed and similar applied pressure, the fibers remain well embedded in the matrix, whilst less pulverization and peeling-off of the fibers takes place on the worn surface. Likewise, the wear track on the steel disk at $p\nu$ -product of 2×3 MPa·m/s is smoother with fewer apparent scratches (Fig. 7d), in contrast with that at $p\nu$ -product of 3×1 MPa·m/s (Fig. 7b). It is noteworthy that there are substantially more sphere-shape debris evenly distributing on the wear track at $p\nu$ -product of 2×3 MPa·m/s, as shown in Fig. 7d. The debris (presumably TiO₂ wrapped by PPS), which act in a rolling fashion, is considered

to be one of main factors that reduce the friction coefficient as well as severity of wear. Therefore, it is considered that the TiO₂ particles can be released faster at an appropriately high sliding speed. This may enhance the positive rolling effect, which provides a lasting protection to the worn surface from the aggressive damage by the hard asperity tips of counterpart.

6 Conclusions

1. The application of artificial neural network technology permitted to analyze the wear and friction behavior of the PPS composites filled with short carbon fibers and sub-micro TiO₂ particles. The ANN prediction and the experimental observation show a good agreement.
2. A synergistic effect of the two fillers on improving the wear resistance was reported. The lowest specific wear rate of approximately 4.0×10^{-7} mm³/Nm was found for PPS with 15 vol.% SCF and 5 vol.% TiO₂. A more optimal composition of PPS with 15 vol.% SCF and 6 vol.% TiO₂ was estimated by ANN prediction.
3. The possible interaction of short carbon fibers and TiO₂ could be interpreted in terms of a positive rolling action of sub-micro TiO₂ particles, which protected the short carbon fibers from being pulled-out from the matrix by the counterpart asperities and finally resulted in an enhanced wear resistance of the composites.
4. Sliding speed and applied pressure have their respective influence on the wear of PPS with 15 vol.% SCF and 5 vol.% TiO₂. Under higher *p**v*-conditions, the increase in sliding speed results in a relative milder increase of depth wear rate in comparison to that in applied pressure. The phenomenon indicates that a combination of appropriately high sliding speed and applied pressure can augment the hybrid reinforcement effect of the two fillers and develop a compact and smooth transfer film, and consequently reduce the severity of wear.

Acknowledgement

The authors gratefully acknowledge the financial support of the German Research Foundation (DFG FR 675/45-1: Wear prediction of polymers and composites using an artificial neural network approach). We would like to thank F. Richter (Ensinger GmbH, Germany) and Dipl.-Ing. B. Lehmann (IVW, Germany) for their assistance in experiments. Dr. G. Zhang (IVW, Germany) is appreciated for his valuable discussions. K. Friedrich is grateful to the Australian Research Council for his International

References

- [1] Palabiyik M, Bahadur S. Tribological studies of polyamide 6 and high-density polyethylene blends filled with PTFE and copper oxide and reinforced with short glass fibers. *Wear* 2002;253(3-4):369-376.
- [2] Sviridyonok AI. Self lubrication mechanism in polymer composites. *Tribol Int* 1991;24(1):37-43.
- [3] Tewari US, Bijwe J. Recent development in tribology of fibre reinforced composites with thermoplastic and thermosetting matrices. In: Friedrich K, editor. *Advances in composite technology*, Amsterdam: Elsevier, 1993, p. 159-207.
- [4] Bucher J. Polyphenylene Sulfide. *Plastics World* 1997;5:53.
- [5] Fred JR. *Polymer science and technology*. New York: Pearson Education, 2003.
- [6] Lhymn C, Bozolla J. Friction and wear of fiber reinforced PPS composites. *Adv Polym Tech* 1987;7(4):451-461.
- [7] Yu L, Bahadur S, Xue Q. An investigation of the friction and wear behaviors of ceramic particle filled polyphenylene sulfide composites. *Wear* 1998;214(1):54-63.
- [8] Yu L, Yang S, Liu W, Xue Q. An investigation of the friction and wear behaviors of polyphenylene sulfide filled with solid lubricants. *Polym Eng Sci* 2000;40(8):1825-1832.
- [9] Zhao Q, Bahadur S. A study of the modification of the friction and wear behavior of polyphenylene sulfide by particulate Ag_2S and $PbTe$ fillers. *Wear* 1998;217(1):62-72.
- [10] Zhao Q, Bahadur S. The mechanism of filler action and the criterion of filler selection for reducing wear. *Wear* 1999;225-229:660-668.
- [11] Schwartz CJ, Bahadur S. The role of filler deformability, filler-polymer bonding, and counterface material on the tribological behavior of polyphenylene sulfide (PPS). *Wear* 2001;251(1-12):1532-1540.
- [12] Cho MH, Bahadur S, Pogolian AK. Friction and wear studies using Taguchi method on polyphenylene sulfide filled with a complex mixture of MoS_2 , Al_2O_3 , and other compounds. *Wear* 2005;258(11-12):1825-1835.
- [13] Schwartz CJ, Bahadur S. Studies on the tribological behavior and transfer film-counterface bond strength for polyphenylene sulfide filled with nanoscale alumina particles. *Wear* 2000;237(2):261-273.

- [14] Bahadur S, Sunkara C. Effect of transfer film structure, composition and bonding on the tribological behavior of polyphenylene sulfide filled with nano particles of TiO₂, ZnO, CuO and SiC. *Wear* 2005;258(9):1411-1421.
- [15] Bahadur S. The development of transfer layers and their role in polymer tribology. *Wear* 2000;245(1-2):92-99.
- [16] Zhang Z, Friedrich K. Tribological characteristics of micro- and nanoparticle filled polymer composites. In: Friedrich K, Fakirov S, Zhang Z, editors. *Polymer Composites: From Nano- to Micro- Scale*, New York: Springer, 2005, p. 169-185.
- [17] Chang L, Zhang Z, Zhang H, Friedrich K. Effect of nanoparticles on the tribological behaviour of short carbon fibre reinforced poly(etherimide) composites. *Tribol Int* 2005;38(11-12):966-973.
- [18] Chang L, Zhang Z, Breidt C, Friedrich K. Tribological properties of epoxy nanocomposites Part II. A combinative effect of short carbon fibre with nano-TiO₂. *Wear* 2006;260(7-8):869-878.
- [19] Cho MH, Bahadur S. Study of the tribological synergistic effects in nano CuO-filled and fiber-reinforced polyphenylene sulfide composites. *Wear* 2005;258(5-6):835-845.
- [20] Zeng P. Neural computing in mechanics. *Applied Mechanics Reviews* 1998;51(2):173-197.
- [21] Zhang Z, Friedrich K. Artificial neural networks applied to polymer composites: a review. *Compos Sci Technol* 2003;63(14):2029-2044.
- [22] Kadi HE. Modeling the mechanical behavior of fiber-reinforced polymeric composite materials using artificial neural networks-A review. *Compos Struct* 2006;73(1):1-23.
- [23] Haykin S. *Neural networks: a comprehensive foundation*. Upper Saddle River: Prentice Hall, 1999.
- [24] Jiang Z, Zhang Z, Friedrich K. Prediction on Wear Properties of Polymer Composites with Artificial Neural Networks. *Compos Sci Technol* 2007;67(2):168-176.
- [25] Jiang Z, Zhang Z, Gyurova L, Friedrich K. Neural Network Based Prediction on Mechanical and Wear Properties of Short Fibers Reinforced Polyamide Composites. *Mater Design* 2007:In press.
- [26] Demuth H, Beale M. *Neural network toolbox: for use with MATLAB (Version 4.0)*.

The MathWorks, Inc., 2004.

[27] Friedrich K, Zhang Z, Schlarb AK. Effects of various fillers on the sliding wear of polymer composites. *Compos Sci Technol* 2005;65(15-16):2329-2343.

[28] Jain VK. Investigation of the wear mechanism of carbon-fiber-reinforced acetal. *Wear* 1983;92(2):279-292.

[29] Xian G, Zhang Z. Sliding wear of polyetherimide matrix composites I. Influence of short carbon fiber reinforcement. *Wear* 2005;258(5-6):776-782.

[30] Friedrich K. Wear of reinforced polymers by different abrasive counterparts. In: Friedrich K, editor. *Friction and wear of polymer composites*, Amsterdam: Elsevier, 1986, p. 233-287.

[31] Rapoport L, Lvovsky M, Lapsker I, Leshinsky V, Volovik Y, Feldman Y, Zak A, Tenne R. Slow release of fullerene-like WS₂ nanoparticles as a superior solid lubrication mechanism in composite matrices. *Adv Eng Mater* 2001;3(1-2):71-75.

Captions of figures

Fig. 1. A schematic illustration of the artificial neural network.

Fig. 2. Measured and predicted (a) specific wear rate and (b) friction coefficient vs. the

content of TiO₂ particles for the PPS composites with different content of short carbon fibers. The measured data points with error bars are shifted along X-axis to the right side for a clearer display.

Fig. 3. ANN predicted 3D profiles of (a) the specific wear rate, (b) the friction coefficient as function of the sliding speed and applied pressure for PPS with 15 vol.% SCF and 5 vol.% TiO₂. The measured data are plotted as black points with error bars.

Fig. 4. Measured and predicted depth wear rate as a function of pv -product. A quasi-linear increase trend can be observed.

Fig. 5. SEM micrographs of the worn surfaces under standard test conditions (sliding speed = 1 m/s, applied pressure = 1 MPa) for (a) PPS with 15 vol.% SCF, (b) PPS with 5 vol.% TiO₂, (c) PPS with 15 vol.% SCF and 5 vol.% TiO₂. The arrows in the top-left corner indicate the sliding direction of the pin.

Fig. 6. Illustration of the rolling effect of sub-micro-particles protecting the short carbon fibers. (a) A whole view. (b) Matrix-wrapped particles roll on the matrix, and reduce the abrasion of matrix. (c) Particles prevent the counterpart tip from directly scraping the fiber. However, the debris ploughed by the tip are blocked by the exposed fiber and accumulate nearby. (d) Particles act as an abrasive component to polish the fiber surface. (e) The counterpart tip moves through the fiber surface, sometimes result in the damage of fiber edge.

Fig. 7. SEM micrographs of PPS with 15 vol.% SCF and 5 vol.% TiO₂: (a) worn surface and (b) wear track at 3×1 MPa·m/s; (c) worn surface and (d) wear track at 2×3 MPa·m/s. The arrows on the top-left corner indicate the sliding direction of the pin.

Table 1

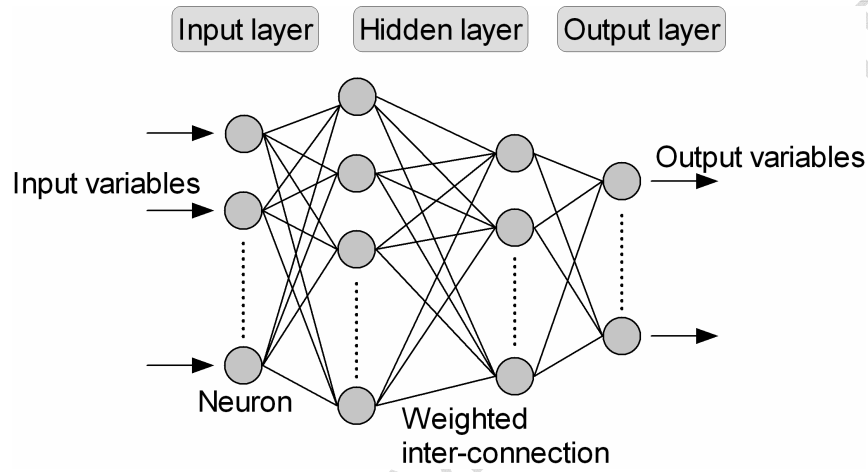
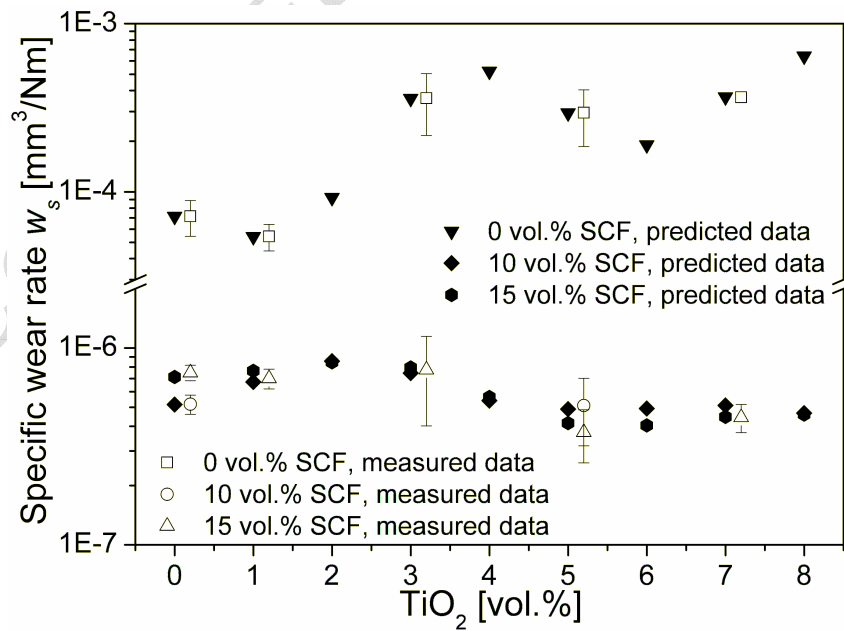
Measured parameters for input and output of ANN.

Input				
Material compositions	PPS matrix (65-100 vol.%)	Short carbon fiber (0, 10, 15 vol.%)	Nano-TiO ₂ particle (0, 1, 3, 5, 7 vol.%)	Lubricant PTFE (0, 5, 10 vol.%) Graphite (0, 5, 10 vol.%)
Testing conditions	Sliding speed (1, 3 m/s)	Applied pressure (1, 2, 3 MPa)		
Output				

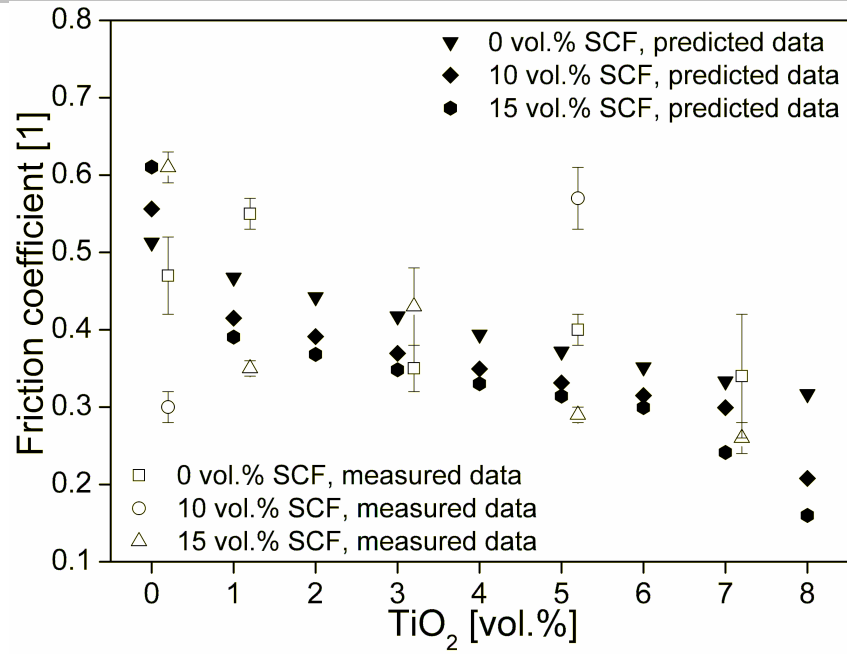
Table 2

Maximum contact temperature of PPS with 15 vol.% SCF and 5 vol.% TiO₂ at different pV -products.

pV -product [MPa·m/s]	1	2	3	3	6	9
Sliding speed [m/s]	1	1	1	3	3	3
Applied pressure [MPa]	1	2	3	1	2	3
Maximum contact temperature [°C]	45.0	47.3	54.6	57.5	113.9	120.1

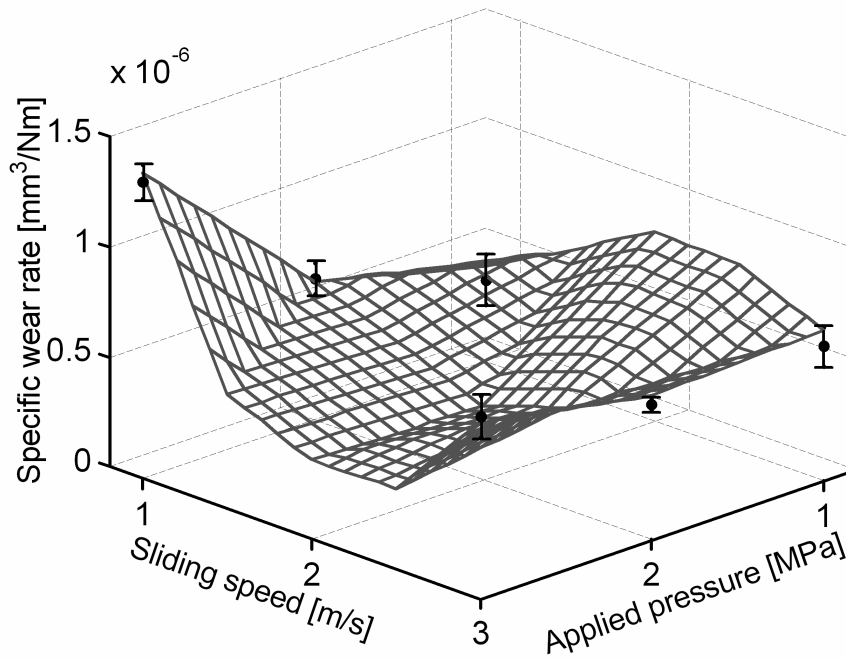
**Fig. 1.** A schematic illustration of the artificial neural network.

(a)

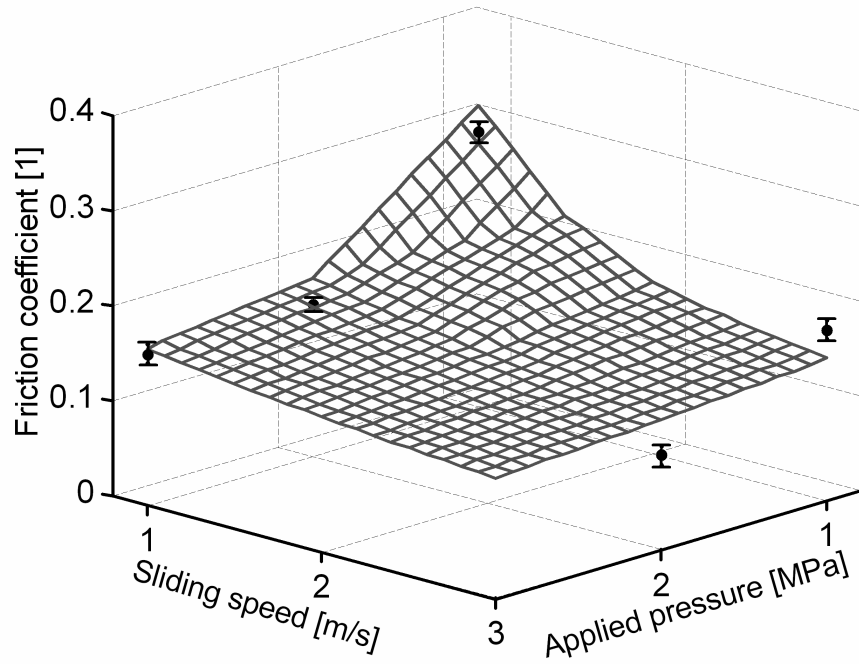


(b)

Fig. 2. Measured and predicted (a) specific wear rate and (b) friction coefficient vs. the content of TiO₂ particles for the PPS composites with different content of short carbon fibers. The measured data points with error bars are shifted along X-axis to the right side for a clearer display.



(a)



(b)

Fig. 3. ANN predicted 3D profiles of (a) the specific wear rate, (b) the friction coefficient as function of the sliding speed and applied pressure for PPS with 15 vol.% SCF and 5 vol.% TiO₂. The measured data are plotted as black points with error bars.

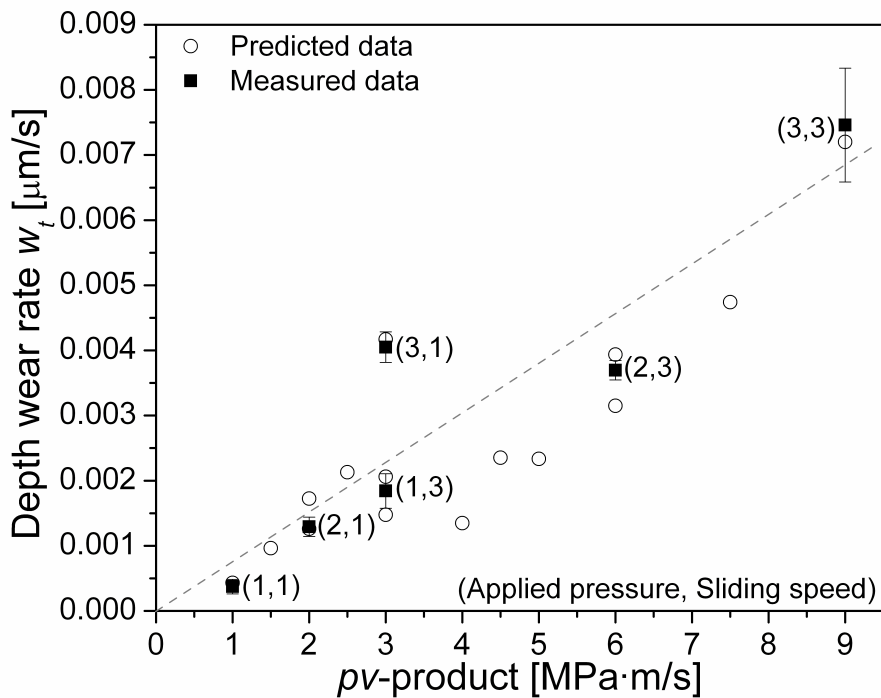
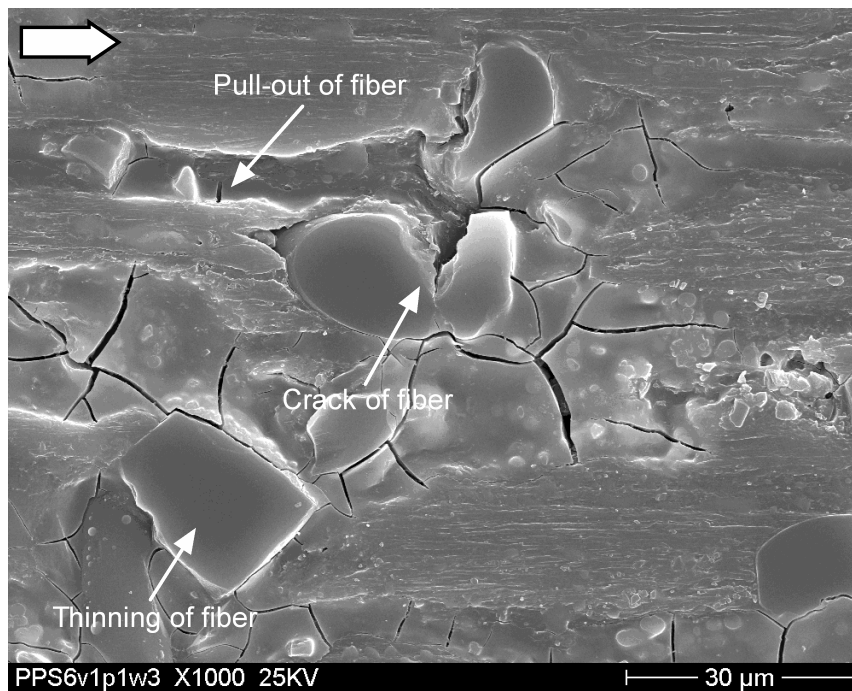
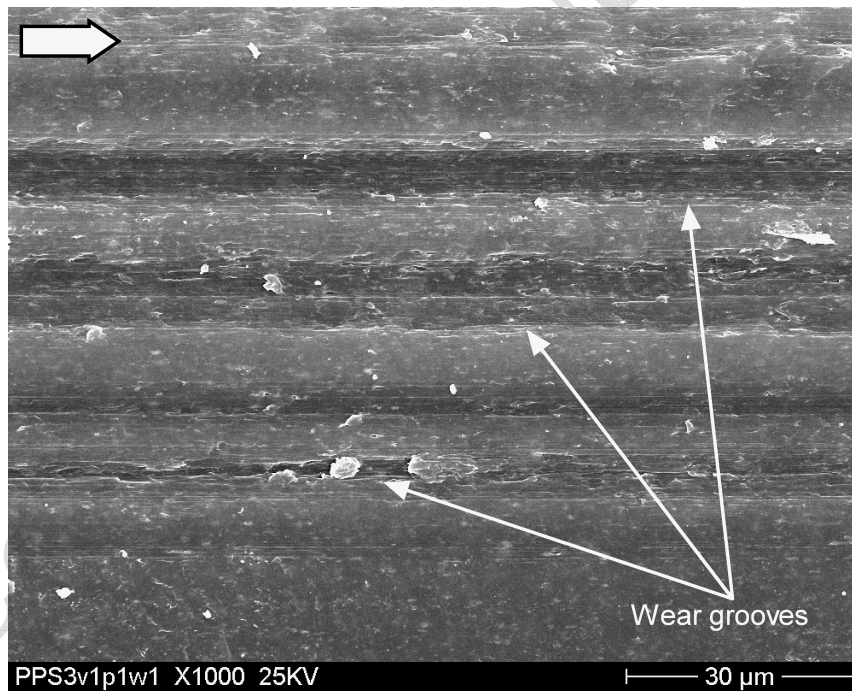


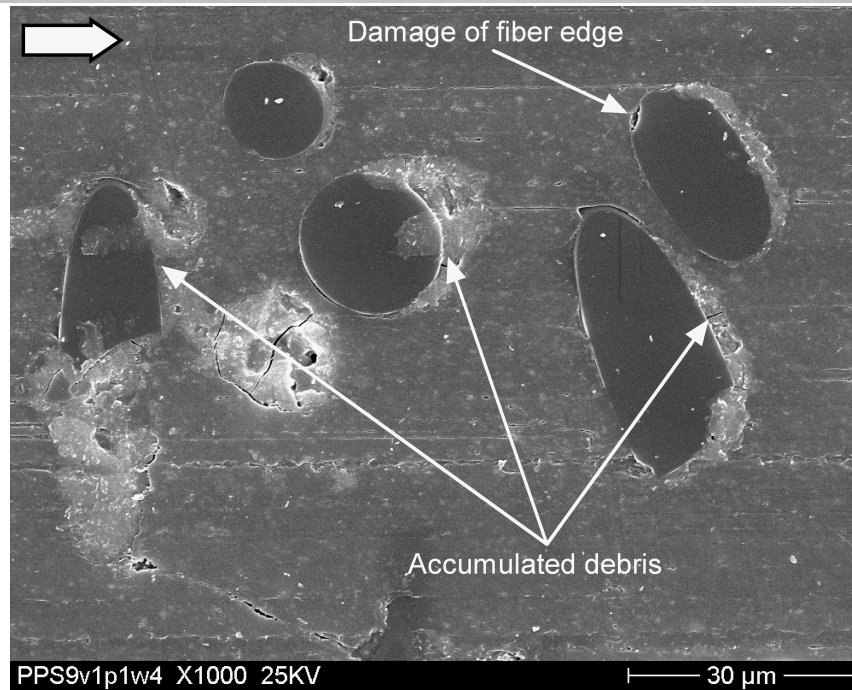
Fig. 4. Measured and predicted depth wear rate as a function of pv -product. A quasi-linear increase trend can be observed.



(a)

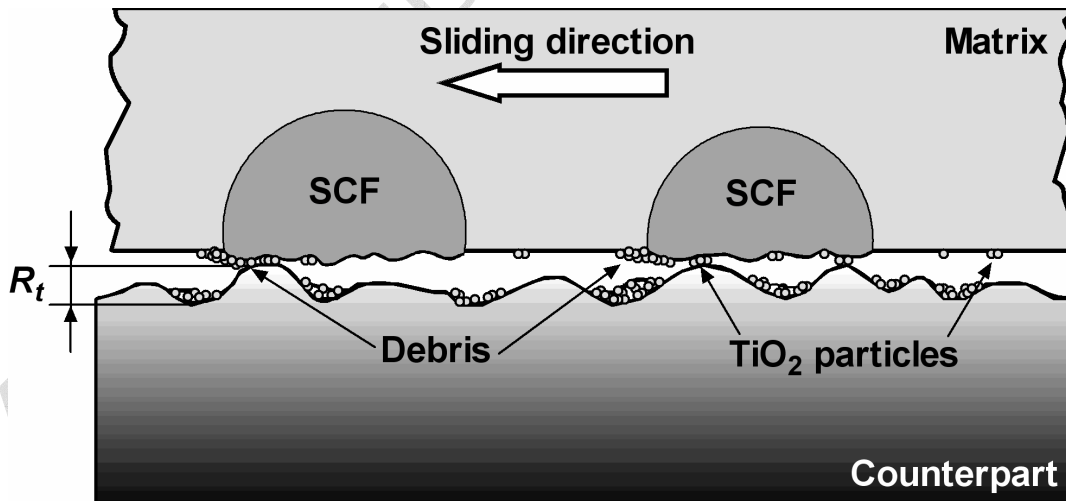


(b)



(c)

Fig. 5. SEM micrographs of the worn surfaces under standard test conditions (sliding speed = 1 m/s, applied pressure = 1 MPa) for (a) PPS with 15 vol.% SCF, (b) PPS with 5 vol.% TiO₂, (c) PPS with 15 vol.% SCF and 5 vol.% TiO₂. The arrows in the top-left corner indicate the sliding direction of the pin.



(a)

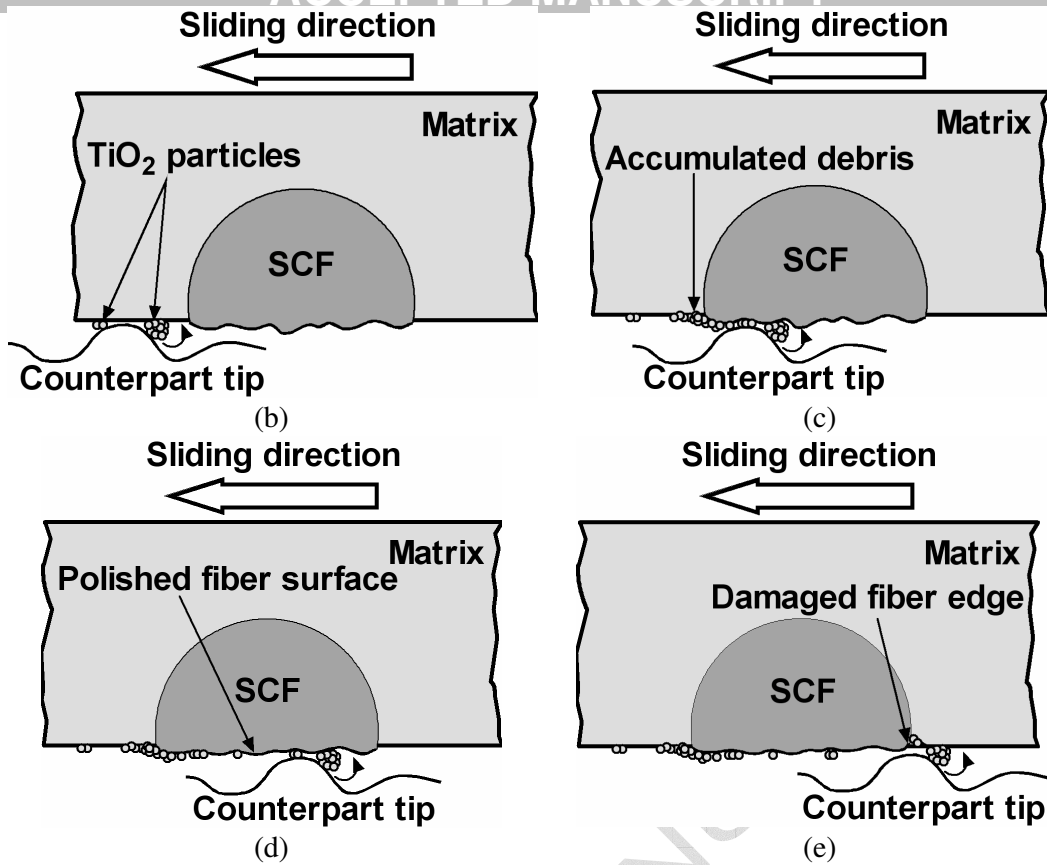
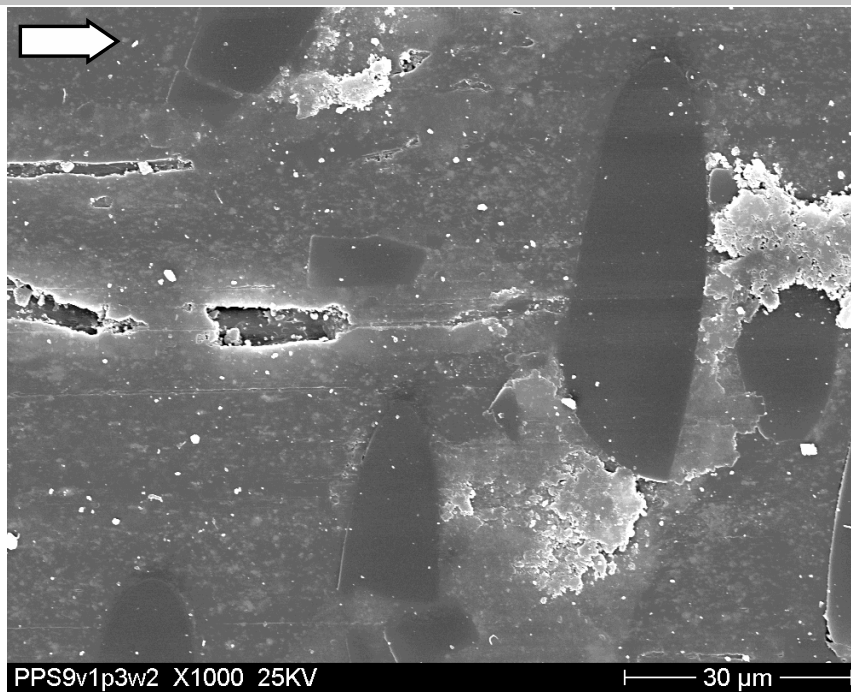
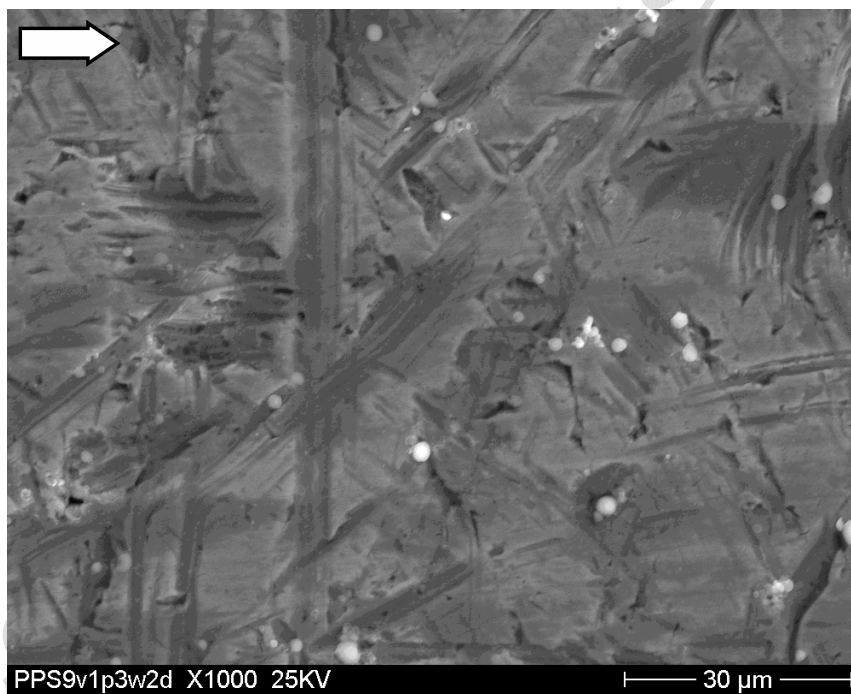


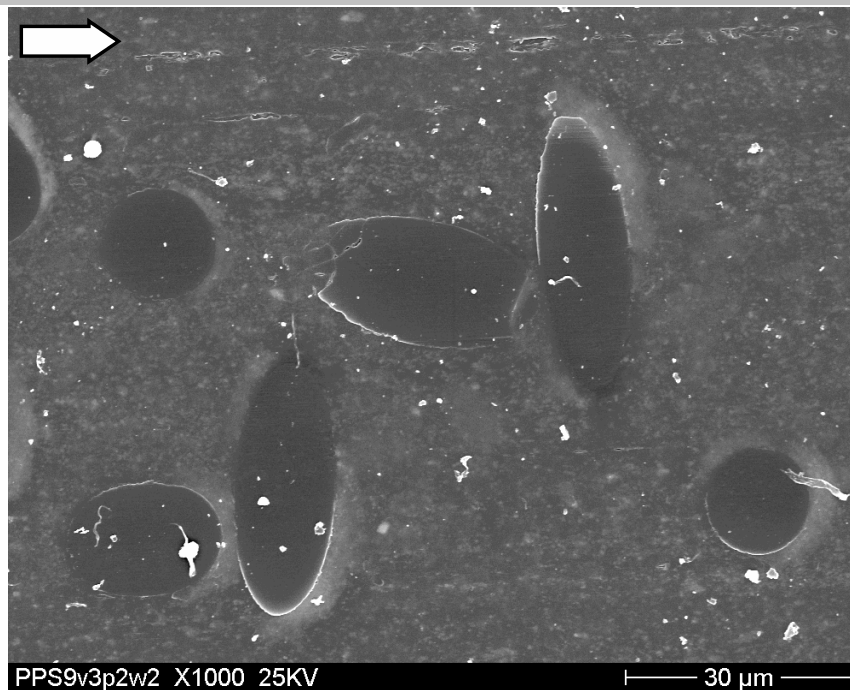
Fig. 6. Illustration of the rolling effect of sub-micro-particles protecting the short carbon fibers. (a) A whole view. (b) Matrix-wrapped particles roll on the matrix, and reduce the abrasion of matrix. (c) Particles prevent the counterpart tip from directly scraping the fiber. However, the debris ploughed by the tip are blocked by the exposed fiber and accumulate nearby. (d) Particles act as an abrasive component to polish the fiber surface. (e) The counterpart tip moves through the fiber surface, sometimes result in the damage of fiber edge.



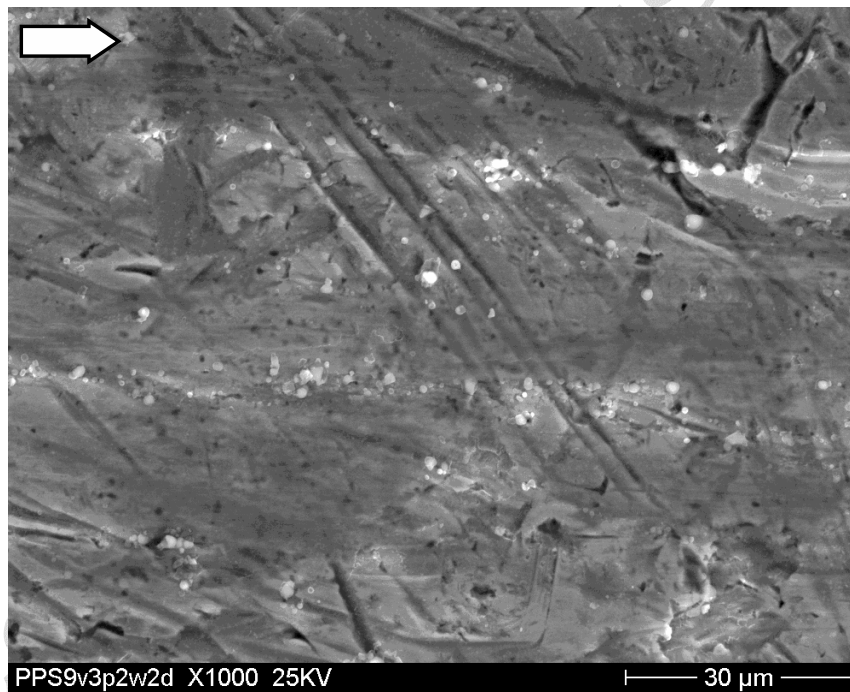
(a)



(b)



(c)



(d)

Fig. 7. SEM micrographs of PPS with 15 vol.% SCF and 5 vol.% TiO₂: (a) worn surface and (b) wear track at 3×1 MPa·m/s; (c) worn surface and (d) wear track at 2×3 MPa·m/s. The arrows on the top-left corner indicate the sliding direction of the pin.s